



ORGANIC
CHEMISTRY
FRONTIERS

Metal-Free Cross-Coupling of n -Conjugated Triazenes with Unactivated Arenes via Photoactivation

Journal:	<i>Organic Chemistry Frontiers</i>
Manuscript ID	QO-RES-08-2018-000938.R1
Article Type:	Research Article
Date Submitted by the Author:	17-Oct-2018
Complete List of Authors:	Barragan, Horacio; University of Texas at Arlington Noonikara, Anurag; University of Texas at Arlington Yang, Chou-Hsun; University of Colorado Denver, Chemistry WANG, Haobin; University of Colorado Denver, Chemistry; Bugarin, Alejandro; University of Texas at Arlington, Department of Chemistry & Biochemistry

SCHOLARONE™
Manuscripts



Metal-Free Cross-Coupling of π -Conjugated Triazenes with Unactivated Arenes via Photoactivation

Enrique Barragan,^a Anurag Noonikara-Poyil,^a Chou-Hsun Yang,^b Haobin Wang,^{*b} and Alejandro Bugarin^{*a}

Received 00th January 20xx,
Accepted 00th January 20xx

DOI: 10.1039/x0xx00000x

www.rsc.org/

Abstract: Cross-coupling of aryl compounds is one of the most powerful carbon-carbon bond forming reactions available. However, the vast majority employ scarce and expensive transition metal salts, in combination with high temperatures and long reaction times. Herein, we report a new, metal-free biaryl coupling that includes photoactivation of π -conjugated triazenes, in the presence of unactivated arenes, carried out at room temperature. Key experiments and theoretical calculations, to elucidate mechanistic details of this new, direct and significantly milder synthetic approach are presented.

Introduction

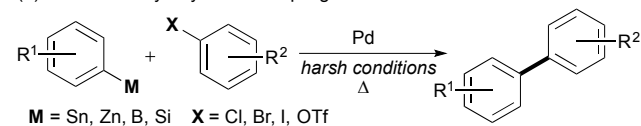
Since its formal discovery and initial development near the turn of the nineteenth century, the science of photochemistry has provided attractive and milder alternatives to traditional thermal reactions.¹⁻³ As early as 1912, major photochemistry pioneer Giacomo Ciamician envisioned a future where human civilization was powered primarily by sunlight.⁴ He also indicated the need to eventually replace fossil fuels with renewable alternatives. In particular, with respect to chemical processes, he recognized that photochemical reactions typically involve milder reaction conditions compared to thermal methods, therefore providing a sustainable alternative.⁴ In general, photons in the ultraviolet and visible regions of the electromagnetic spectrum hold sufficient energy to promote molecules to excited electronic states, which in turn can lead to complementary mechanistic pathways that are inaccessible to molecules in the ground state.⁵ For example, chemists around the globe have achieved a multitude of challenging transformations, under mild photochemical conditions, that are often impossible without the use of high temperatures or aggressive reagents, such as oxidations,⁶ isomerizations,⁷ cycloadditions,^{8,9} deprotections,¹⁰ and cross-couplings.¹¹ Among the former, aryl-aryl cross-coupling is one of the most challenging organic transformation in synthetic chemistry.¹² This class of reaction is of paramount value in organic chemistry because they provide access to a variety of valuable chemical scaffolds required to complete syntheses of numerous compounds, including many key biologically-active molecules.¹² Traditionally, aryl-aryl cross-coupling reactions are mostly achieved using Pd-catalysed methods such as: Suzuki,¹³⁻¹⁶ Negishi,¹⁷⁻¹⁹ Stille,^{20,21} or Hiyama^{22,23} couplings (Scheme 1, eq. 1). Although these methods typically provide the desired adducts in high yields, they often involve the use of stoichiometric toxic heavy metals, such as organic Zn or Sn species, which require specialized procedures for their synthesis, purification, recovery, and disposal.²⁴ In addition, signify-

^b Department of Chemistry, University of Colorado Denver, Denver, Colorado, 80217, United States.

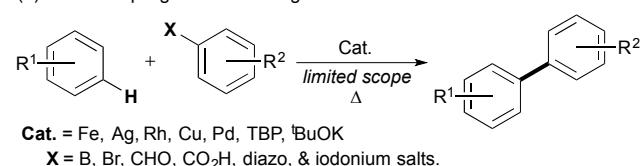
† Footnotes relating to the title and/or authors should appear here.

Electronic Supplementary Information (ESI) available: Experimental details, procedures, ¹H NMR & ¹³C NMR spectra, HRMS, and theoretical calculations see DOI:

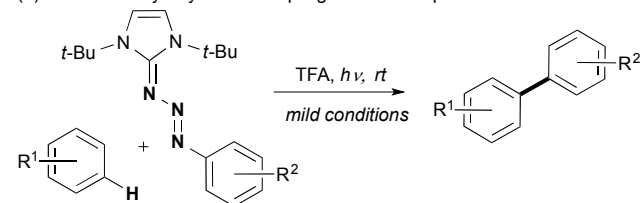
(1) Traditional aryl-aryl cross-coupling reactions:



(2) Cross-coupling reactions using unactivated arenes:



(3) Metal-free aryl-aryl cross-coupling at room temperature: **This work**



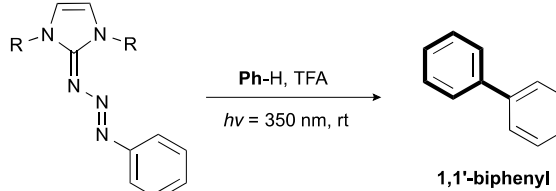
Scheme 1 Representative syntheses of biaryl compounds.

cant major limitations encountered in these transition-metal catalysed cross-coupling reactions are high temperatures, that limit functional group tolerance, and long reaction times, which rise operation costs.²⁵ Alternately, milder synthetic methods, that employ unactivated arenes for the preparation of biaryls, have been reported, albeit still using high temperatures (Scheme 1, eq. 2).²⁶ Among these methods, the most reliable procedures take advantage of highly reactive species such as aryl-iodonium salts,²⁷ aryl-diazotates,²⁸ and aryldiazonium salts²⁸ in the

^a Department of Chemistry and Biochemistry, University of Texas at Arlington, Arlington, Texas 76019, United States. E-mail: bugarin@uta.edu

presence of catalytic amounts of transition metals at high temperatures. Aryl-aryl cross-couplings that take advantage of aryldiazonium salts are perhaps the mildest approach thus far reported since they release molecular nitrogen, as the clean by-product.^{29,30} In addition, aryldiazonium salts are versatile intermediates since they can generate aryl cations^{26,27} or aryl radicals depending on the reaction conditions.³¹ A major disadvantage of aryldiazonium salts is their instability, making them less desirable, specially at large scales since they are known to be explosive.³² Therefore, it is clear that a milder and straightforward approach to aryl-aryl cross-couplings is still highly desired.

Table 1 Optimization of reaction conditions^a



Entry	R	TFA (equiv.)	Time (h)	Yield (%) ^b
1	Me	1	1	7
2	Me	1	2	18
3	Me	1	4	20
4	Me	1	24	22
5	Me	0.1	2	traces
6	Me	2	2	20
7	Me	5	2	31
8	Me	10	2	33
9	<i>t</i> -Bu	5	2	59
10 ^c	<i>t</i> -Bu	5	2	3
11 ^d	<i>t</i> -Bu	5	2	0

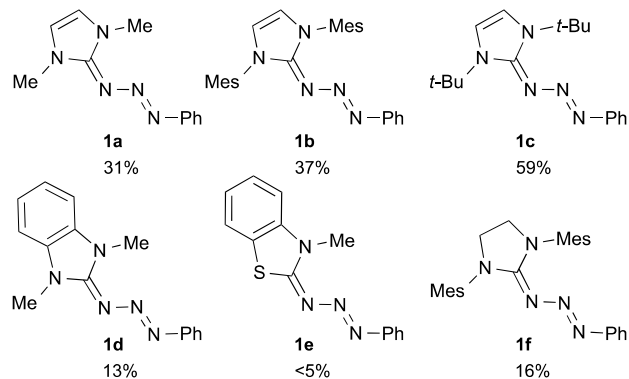
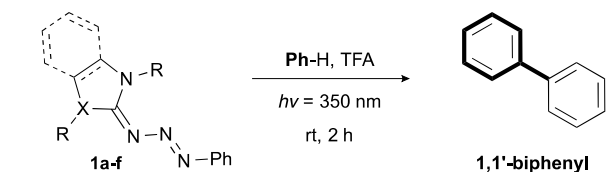
^aReactions were carried out with the corresponding triazene (0.2 mmol, 1 equiv) and TFA in 2 mL of benzene in a quartz tube under UV irradiation (350 nm). ^bIsolated yields by silica gel flash column chromatography. ^cReaction carried, under dark, at 65 °C. ^dReaction carried out under dark at room temperature.

The present study involves a continuation of our work on the elucidation of the inherited reactivity of π -conjugated triazenes³³⁻³⁵ with a particular emphasis on their capability of providing *in situ* generation of aryldiazonium salts, thus avoiding potential explosions, while maintaining mild reaction conditions. Herein, we report π -conjugated triazenes as aryldiazonium reservoirs³⁶ that can be delivered under photoirradiation at room temperature to produce biaryl adducts, in short reaction times. In this work, we take advantage of our previous observation that Brønsted acids can increase the reactivity π -conjugated triazenes³⁶ and Jewett's report on photoisomerization of triazenes.³⁷⁻³⁹ This work also includes mechanistic studies, including detailed theoretical calculations, to determine if cationic, radical, or *ipso* substitution is responsible for the observed reactivity of this metal-free aryl-aryl cross coupling that eliminates several of the earlier mentioned shortcomings.

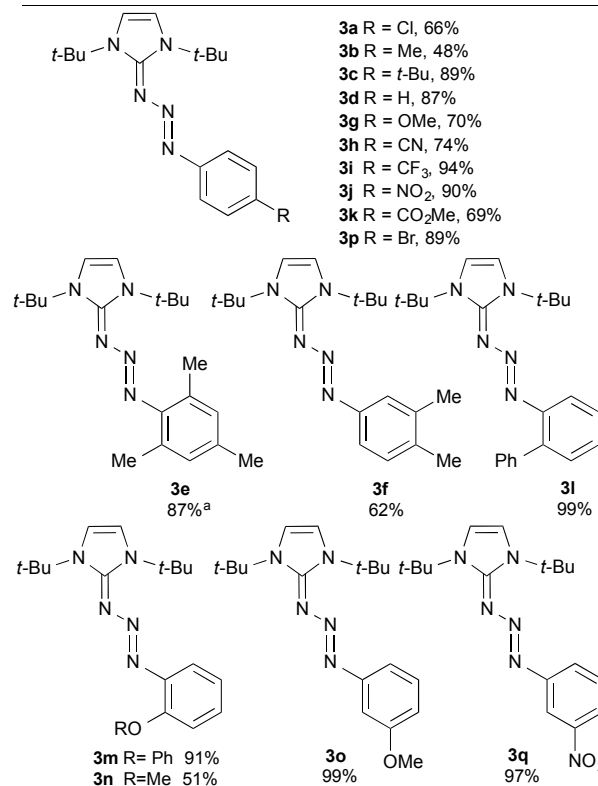
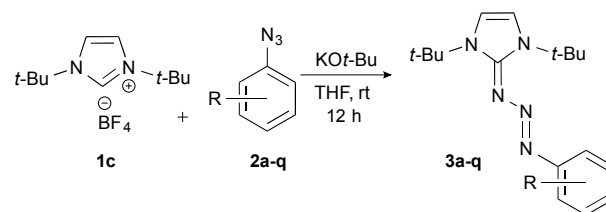
Results and discussion

Initially, we investigated the conversion of two π -conjugated triazenes derived from methyl and *tert*-butyl imidazolium salts into 1,1'-biphenyl (Table 1). In order to find the best reaction conditions, the photochemical transformation was studied using different Brønsted acids and the impact that time and Brønsted acid's stoichiometry have on the product yield. From these experiments, trifluoroacetic acid (TFA) was identified as a superior catalyst over other acids such as: HCl, TsOH, H₂SO₄, and AcOH that only generated small amounts of the desired biaryl product (not shown). With TFA as the optimal Brønsted acid on hand, the reaction time was studied, using 1.0 equivalents of TFA (Table 1, entries 1-4). From these results, it was noticed that the reaction virtually halt after 2 h (entry 2), with relatively small increments up to reaction times of 24 h (entries 3 and 4). Therefore, 2 h was selected as a satisfactory reaction time for this transformation. Optimization of TFA's stoichiometry in the reaction media was then investigated using 0.1 to 10 equivalents of TFA (entries 5 to 8). A catalytic amount (0.1 equiv) of TFA, resulted in only trace amount of product formation (entry 5), while the maximum yield (33%) was observed using 10 equiv. (entry 8). However, since using lower TFA loading (5 equiv.) led to an essentially similar yield (31%), this latter amount was employed as a preferred loading (entry 7). Subsequently, using a different triazene derived from *di*-*tert*-butylimidazolium tetrafluoroborate (**1c**), we observed a substantial increase in yield (59%) (entry 9). The reaction was also performed under thermal conditions (65°C) without UV irradiation, affording the expected product in only 3% yield, thus highlighting the power of photochemical induction (entry 10). Also, as a control experiment, we ran the reaction at room temperature, without applying heat or UV irradiation, under which conditions no product was obtained (entry 11), thereby providing additional support for the need of photoactivation to produce the desired adduct.

With the best starting conditions on hand, and aware of the potential effect of the triazene structure on reaction yields, we synthesized more triazenes using different *N*-heterocyclic carbene (NHC) precursors and azidobenzene to evaluate their effectiveness for the cross-coupling reaction (Scheme 2). As depicted in Scheme 2, reaction yields are highly dependent on the stability of the triazenes.³³⁻³⁵ For example, the highly stable triazene **1f** doesn't react well under these reaction conditions (16%). On the other hand, highly unstable triazenes **1d** and **1e** decomposed too quickly into many by-products, affording the expected product in low yield, 13% and <5%, respectively. Importantly, we also synthesized triazenes that possess moderate stability (**1a-c**), which release the phenyldiazonium ion slow enough to be captured by the unactivated arene. The yields of triazenes **1a-c** are proportional to the size of the nitrogen substituents on the imidazolium moiety, going from 31% for



Scheme 2 NHC precursors' optimization. Reaction conditions: triazene (0.2 mmol, 1 equiv), TFA (1.0 mmol, 0.1 mL, 5 equiv) in 2 mL of benzene in a quartz tube under UV irradiation (350 nm) for 2 h. All yields are of isolated materials.



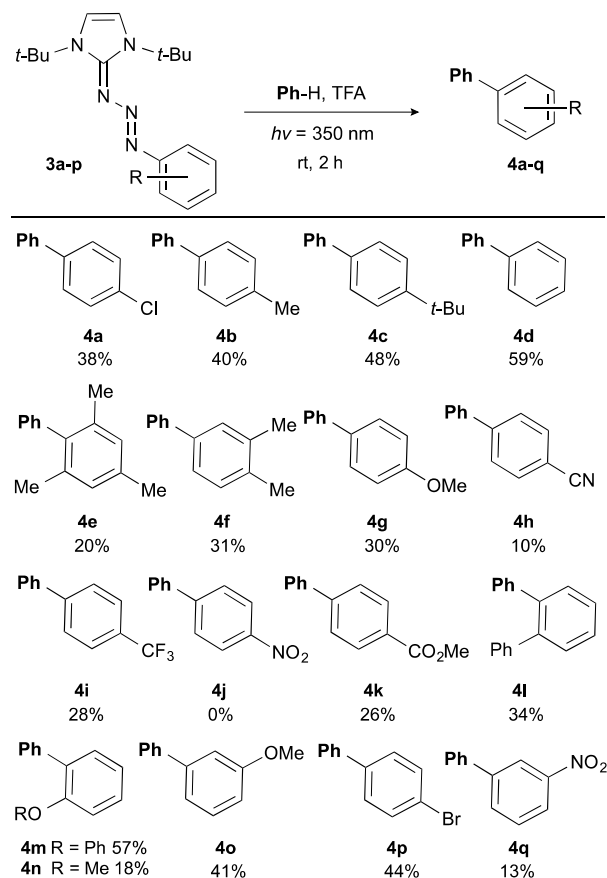
Scheme 3 Synthesis of π -conjugated triazenes. Reaction conditions: Di*tert*-butylimidazolium tetrafluoroborate (2 mmol, 540 mg, 1 equiv), aromatic azide (2 mmol, 1 equiv), potassium *tert*-butoxide (2.4 mmol, 269 mg, 1.2 equiv) in 10 mL of THF at room temperature for 12 h. ^aNaH was used as base instead of KO*t*-Bu. All yields are from isolated materials.

methyl (**1a**), 37% for mesityl (**1b**), to a significantly higher yield of 59% for *tert*-butyl (**1c**). This trend is perhaps due to increased steric interactions between the nitrogen substituents and the phenyl moiety that develop during the triazene *E/Z* isomerisation upon photo-irradiation, making the triazene derived from **1c** the best choice for this aryl-aryl coupling.³⁰

Having identified *tert*-butylimidazolium tetrafluoroborate (**1c**) as the most effective NHC partner, we proceeded to synthesize several π -conjugated triazenes by reacting the NHC precursor **1c** with miscellaneous aromatic azides, following our previously established protocol,³³ to afford seventeen new triazenes **3a-3q** with good to excellent yields (Scheme 3). This relatively large set of triazenes includes, electron-donating and electron-withdrawing substituents. In addition, steric hindrance was also considered. For this purpose, we prepared *para*, *ortho*, and *meta* substituted triazenes with yields up to

99% (see Scheme 3). Interestingly, synthesis of triazene **3e** required the use of sodium hydride instead of the commonly used potassium *tert*-butoxide. This observation suggests that the extra benzylic protons in the mesityl moiety further react with *t*-BuOK via radicals,⁴⁰ whereas NaH doesn't.

To study the scope and limitations of the aryl-aryl cross-coupling reaction, the freshly prepared triazenes (**3a-q**) were subjected to UV-irradiation (350 nm) for 2 h periods (Scheme 4). Data obtained from these experiments suggest that the electronic character of the substituents on the phenyl ring of the triazene profoundly influence the reaction yield. The neutral triazene **4d** gave the highest yield (59%), whereas triazenes bearing weak electron-withdrawing or weak electron-donating groups such as: alkyl (**4b** & **4c**) or halides (**4a** & **4p**) afforded moderate yields. In addition, triazenes possessing strong electron-withdrawing groups through resonance afforded lower yields. For example, 4-cyanobiphenyl triazene (**4h**), gave only 10% yield and 4-nitrobiphenyl triazene (**4j**) did not react at all, and nearly stoichiometric amount of unreacted starting material, triazene **3j**, was recovered (Scheme 4). This observation is in agreement with our previous observations³³ and Bielawski,⁴¹ who reported that electron-poor triazenes are particularly stable. This stability renders such triazenes unreactive under our reaction conditions. On the other hand, electron-rich triazenes are highly reactive and readily undergo decomposition to side products, which accounts for the low yield (18%) of 2-methoxybiaryl **4n**. However, increasing the size of the triazene from 2-methoxy (**3n**) to 2-phenoxy (**3m**) increases its stability due to steric effects, while keeping similar electronic effects, thus helping afford bisaryl adduct **4m** in a higher yield (57%). Finally, we were pleased to see that the highly steric hindered triazene (**3e**), afforded the product (**4e**), albeit in 20% yield.

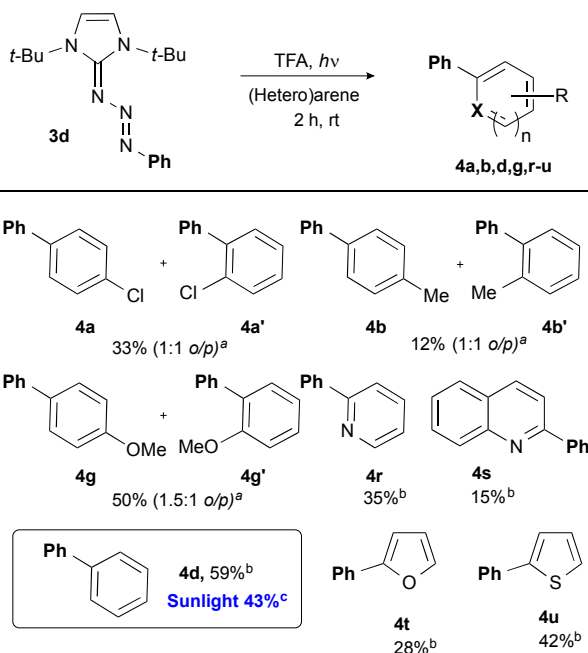


Scheme 4 Synthesis of biphenyls from π -conjugated triazenes. Reaction conditions: Triazene (0.2 mmol, 1 equiv), TFA (1.0 mmol, 0.1 mL, 5 equiv) in 2 mL of benzene in a quartz tube under UV irradiation (350 nm) for 2 h. All yields are from isolated materials.

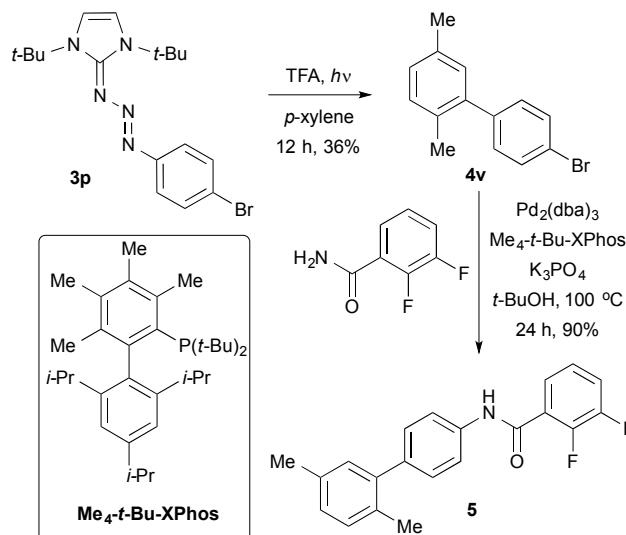
It is speculated that the low yield of **4a** is due to the higher energy required for nucleophilic attack by benzene, on the inaccessible carbocation intermediate (see Table S6[†]). Although, most of the yields are moderated, it is worth noting that the reaction tolerates different functional groups including; halides (Cl & Br), electron-poor (CF₃, NO₂, CO₂Me, & CN), electron-rich (OMe & OPh), and hindered substrates such as mesityl triazene and *ortho* substituted triazenes (Me, OMe & OPh), and most important, none of the substrates produced additional regioisomers (Scheme 4).

To further evaluate the general applicability of this transformation, two different sets of arenes were selected; (1) substituted arenes to investigate their regioselectivity, and (2) heteroarenes, to check its suitability for the preparation of heteroaromatic biaryls, an often-challenging task (Scheme 5).²⁸ Arenes such as chlorobenzene and toluene showed product formation but no regioselectivity (1:1, *o/p*), whereas anisole exhibited some preference for the most nucleophilic position, the *ortho* regioisomer **4g** (1.5:1, *o/p*). In terms of the following heteroarenes: pyridine, quinoline, furan, and thiophene the outcome was encouraging since all the products were isolated, as single regioisomers, albeit in moderate yields (Scheme 5). The observed regioselectivity towards *ortho* and *para* positions, with no *meta* product formed suggests that there is a phenyl cation, derived from the

1 triazene, formed during the reaction steps, and it is in agreement with
 2 the know selectivity of electrophilic aromatic substitutions.⁴² However,
 3 the adducts isolated from heteroarenes suggest that a phenyl radical is
 4 also plausible, since 2-phenylquinoline **4s** was observed (Scheme 5).
 5 Because of the two potential mechanistic pathways, we investigated
 6 both possibilities further and the details are presented below. Of
 7 significant relevance, we note that our transformation can also be
 8 performed under even milder conditions using sunlight in lieu of UV-
 9 radiation. For example, the biphenyl adduct **4d** was obtained in 43%
 10 yield (as highlighted in scheme 5).



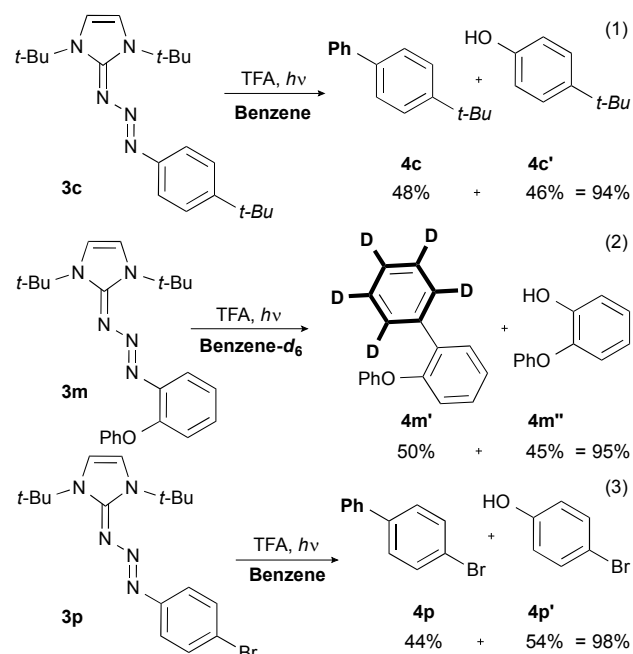
34 **Scheme 5** Synthesis of biphenyls and heterobiaryls. Reaction conditions: Triazene (0.2
 35 mmol, 60 mg, 1 equiv), TFA (1.0 mmol, 0.1 mL, 5 equiv) in 2 mL of the corresponding solvent
 36 in a quartz tube under UV irradiation (350 nm) for 2 h. ^a ¹H NMR yields of the isomeric
 37 mixture, using DMF as internal standard. ^b Isolated yields. ^c The reaction was stirred under
 38 natural sunlight during 9 h.



58 **Scheme 6** Synthesis of immunosuppressant **5**. Reaction conditions: 1. Triazene **3p** (0.5
 59 mmol, 180 mg, 1 equiv), TFA (2.3 mmol, 0.2 mL, 5 equiv) in 2 mL of *p*-xylene in a quartz tube
 60 under UV irradiation (350 nm) for 12 h. 2. 2,3-difluorobenzamide (0.2 mmol, 40 mg, 1.2
 equiv), Pd₂(dba)₃ (4 mol%, 8 mg), Me₄t-Bu-XPhos (6 mol%, 6 mg), K₃PO₄ (0.3 mmol, 44 mg,
 1.5 equiv) in 2 mL of *t*-BuOH at 100 °C for 24 h. Yield are from isolated materials.

To demonstrate the practical utility of our method to synthesize
 bioactive molecules, the known immunosuppressant compound **5**
 was synthesized in two-steps from stable triazene **3p** (Scheme 6).
 Using our mild reaction conditions, the new brominated biaryl **4v**
 was generated from triazene **3p** and *p*-xylene in 36%. A 12 h
 reaction time was required, for the maximum yield, since *p*-xylene
 is sterically hindered. Subsequently, freshly prepared intermediate
4v was coupled with commercially available 2,3-difluorobenzamide,
 following the reaction conditions previously reported by Greaney,²⁷
 to produce the final compound in 90% yield (Scheme 6).

After analysing all the previous results, and to attempt to gain a
 better understanding of the reaction mechanism, we proceeded to
 search for any by-products present in these reactions (Scheme 7).
 Our objective was to elucidate the somewhat modest yields
 obtained for some of the substrates.

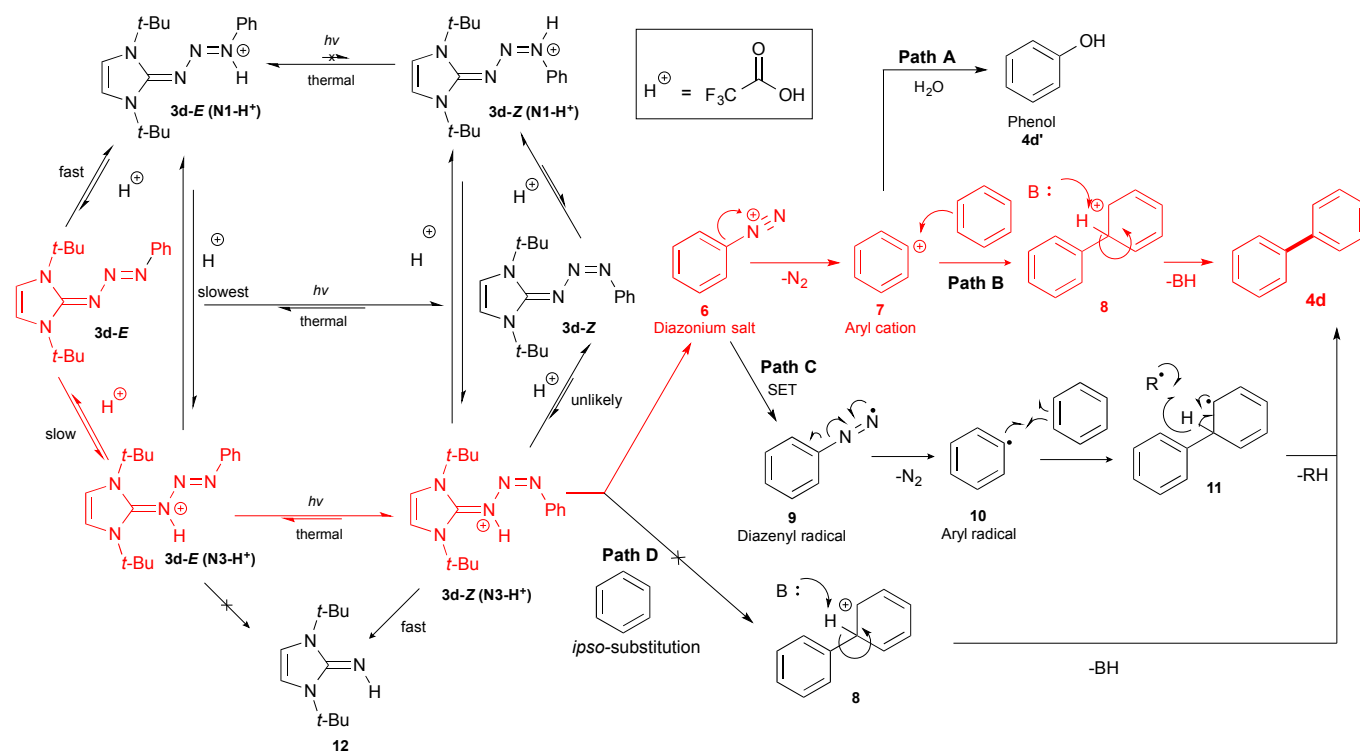


Scheme 7 By-product identification.

For this purpose, we selected three triazenes (**3c**, **3m**, & **3p**) and subjected them to our standard reaction conditions, with the exception that benzene and benzene- d_6 were employed without drying (Scheme 7). To our surprise, phenols **4c'**, **4m''**, and **4p'** were isolated in around 1:1 ratio with respect to the usual biaryl products. The benzene- d_6 experiment helped us to more closely monitor the reaction and revealed that only the expected biaryl product and the phenolic by-product were present in approximating a 1:1 ratio, with a total yield of 95% (Scheme 7, eq. 2). These results indicate that water is competing by capturing the proposed aryl cation that is formed *in situ*. This strongly suggests an ionic mechanism. However, a radical mechanism cannot be ruled out since aryl radicals have been observed during aryldiazonium decomposition.³⁰ After closer analysis of our compiled results, most of the previous reactions presented phenol by-products when wet solvents or reagents were used. However, adding extra water did not affect yields and ratios and our best efforts to perform our reaction under anhydrous conditions did not improve the aryl-aryl cross coupling yields, since minimum amount of water has a profound effect on the phenyl cation intermediate (Fig. 2).

With all experimental information on hand, we proceeded to consider plausible mechanistic pathways that encompass all the observed results (Scheme 8). Additionally, to further explore possible mechanistic pathways, density functional theory (DFT) was employed to examine model compounds discussed in this paper. All of the detailed data obtained from the computational studies can be found in the ESI[†] (Tables S1-S9[†]). All calculations were performed using the quantum chemistry program package Q-Chem 5.0⁴³ with the hybrid functional B3LYP. Geometry optimizations were carried out using the basis set 6-31G* to find the ground state minima. Then, single point electronic energies were obtained using basis set 6-31+G* (i.e., including diffuse functions), whereas test calculations employing a larger basis set 6-311+G** produced relatively smaller differences. Linear response time-dependent DFT (TD-DFT)/TDA calculations were used to calculate the vertical excitation energies and to optimize the excited state structures. Solvent (benzene) effects were approximated using the conductor-like polarizable continuum model (cPCM) model.^{44,45} To gauge the accuracy of the DFT calculations, we also used the auxiliary basis set (resolution-of-identity) second order Møller-Plesset perturbation theory (RI-MP2)⁴⁶⁻⁴⁸ method to calculate ground state energies for all the triazene compounds (Table S1[†]). The benchmark RI-MP2 values are consistent with those from the DFT calculations, suggesting that DFT is adequate for investigating the compounds in this paper.

The first reaction step in Scheme 8 concerns the protonation of 1-*E*, which involves two main possible sites: N1 and N3. Calculations show that the ground state energy of N1-H⁺ is lower than N3-H⁺ for all molecules, as shown in Table S1[†]. As reported in Table S2[†], our calculations, under our experimental conditions, indicate that the neutral molecules have electronic energies lower than the protonated triazenes (N1-H⁺ by 10-20 kcal/mol, and N3-H⁺ by 20-30 kcal/mol). These results were obtained using cPCM model in (dilute) benzene solution, which has a small dielectric constant ($\epsilon=2.27$). On the other hand, the energy differences between the neutral and protonated triazenes are significantly reduced when the solvent dielectric constant is increased. Under the actual experimental condition, where trifluoroacetic acid ($\epsilon=8.55$) is present, favours protonated species to undergo subsequent photoexcitation processes (Tables S3[†]). The minimum energy geometries for the protonated N3-H⁺ and unprotonated triazene complexes in their first bright excited states correspond to 1-*Z* configurations. On the other hand, the protonated N1-H⁺ complexes are still in 1-*E* configurations, which suggest that photoisomerization occurs readily for triazenes protonated on N3, but not for those protonated on N1 (Scheme 8).



Scheme 8 Mechanistic details for the plausible *ipso*, radical, and cationic pathways and the by-product formation. Favoured path in red.

The subsequent reaction step for the photoexcited molecules is the ultrafast internal conversion down to their ground states. In principle the internal conversion competes with the fluorescent decay. To distinguish between the radiative (fluorescent) and non-radiative decay, we estimated the electronic coupling elements (for non-radiative decay) between the ground and excited state using the generalized Mulliken-Hush method (Table S4†).^{49,50} Our calculations indicate that internal conversion is the dominant transition. After the non-radiative internal conversion, the electronic energy is transferred into the vibrational energy of the molecule. The specific partition of the converted energy is determined by the vibronic coupling. Under the linear response approximation, this is represented by the ground state gradient at the geometry of vertical de-excitation. While the magnitude of the force reflects the strength of the vibronic coupling, the direction of it can be used to indicate the reaction coordinate (Fig. 1). Our results show that the vibronic couplings involve primarily the displacement of three nitrogen atoms for the N3-H⁺ complexes, but involve more atoms for N1-H⁺. This suggests that photoexcitation and subsequent internal

conversion facilitate the dissociation reaction for N3-H⁺ with a Z configuration, but not for N1-H⁺ with an E configuration.

At this point in the mechanistic discussion, though the formation of the aryldiazonium intermediate seems plausible, the possibility of direct aromatic *ipso* substitution by the aromatic molecule on the protonated triazene cannot be discarded (Scheme 8, **Path D**). Therefore, to obtain experimental data that would allow us to clarify if *ipso* substitution is part of the mechanism, we attempted the capture of the aryldiazonium intermediate, by means of a Sandmeyer reaction, under our conditions.⁵¹ We subjected triazene **3p** in dichlo-

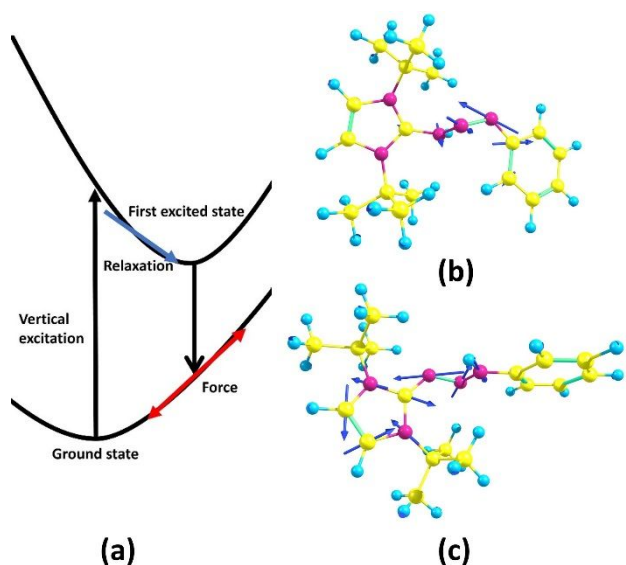


Figure 1 (a) Projection of the force along one normal mode of the ground state equilibrium geometry after internal conversion. The force in the triazene molecules. The arrow stands for the force along with the molecular reaction. (b) and (c) stand for N3-H⁺ and N1-H⁺ of triazene **3d**, respectively.

romethane to reaction with 2.0 equiv of tetrabutylammonium bromide, 1 mol% of CuBr, and 5.0 equiv of TFA under UV irradiation. After 2 h, we observed formation of *p*-dibromobenzene in 23% yield, which supports the presence of the phenyldiazonium intermediate upon photo-activation of the triazene **3p** under acidic conditions, suggesting that *ipso* substitution is not occurring (Scheme 8, path D).

To discuss thermodynamics of forming the expected product in the final reaction step, there are three possible pathways; two for the aryl cation in **Paths A** and **B**, and one for the aryl radical as seen in **Path C** (Scheme 8 and Fig. 2). For A and B pathways, we performed calculations on two complexes, the aryl cation with water and benzene, and compared their binding energies (Table S6[†]). For most species the electronic energy of the aryl cation with water is higher than that with benzene, within a few kcal per mol. This implies that forming the aryl cation with the water complex is slightly more favourable than with the benzene complex (Fig. 2).

We also compared the binding energies between **Path B** and **Path C**, (Table S7[†]). The calculations show that the energy of **Path B** is much lower than **Path C**, by around 40-60 kcal/mol. This indicates that forming the aryl radical complex requires more energy. Therefore, **Path C** is not favourable in the final reaction step. Finally, the energy of final products following **Path A** are slightly higher than **Path B**, within 5 kcal/mol, which indicate that both reactions can occur (Table S8[†], Scheme 8, and Fig. 2).

Finally, we calculated the relative free energies of starting materials, intermediates and products for the aryl-aryl cross-coupling reaction of triazene **3d** (Table S9[†]) and constructed the reaction energy diagram

shown in Figure 2. The total free energy includes the electronic energy, the gas phase entropic contribution and the solvent free energy in the standard state. As can be seen from this diagram, the energies of the ground state protonated triazenes on N1 and N3 are only 15 kcal/mol apart in dilute benzene (and 5 kcal/mol in THF, $\epsilon=7.8$). Under experimental conditions and considering subsequent reactions, the two species are likely in equilibrium with one another. Both the unprotonated triazene **3d-E** and the N1 protonated triazene can be photochemically promoted to their respective excited states, but both relax through non-radiative processes back to the ground state (Fig. 2). On the other hand, once the N3 protonated triazene is promoted to the excited state it will preferentially isomerize to its respective *Z* isomer **3d-Z**, which can then decompose exergonically to the diazonium ion **6** (Fig. 2). From that point, the next reaction intermediate is most likely the aryl cation **7**, since in the presence of solvating water its energy is 17 kcal/mol lower than **6** and 20 kcal/mol lower in benzene (Fig. 2). The possibility of an *ipso* substitution by benzene at this step, instead of the aryl cation formation, cannot be discounted; however, our calculations didn't find it likely. According to existing literature, the true mechanism might lie somewhere in between aryl cation and aryl radical processes.⁴⁷ Finally, the formation of biphenyl **4d** and phenol **4d'** are both likely due to the closeness of their energies, which correlates to the good yields and ratios obtained (Scheme 7).

In summary, the energy of the ground state for N1-H⁺ is more stable than N3-H⁺; the excitation energies of first bright state of deprotonated and protonated triazene complexes are in the ultraviolet region (Table S5[†]). The ultrafast internal conversion for N3-H⁺ in 1-*Z* configuration promotes the subsequent dissociation reaction; whereas for N1-H⁺ there is no such mechanism. The free energies of the aryl cations with water are lower than those with benzene; the free energies of the aryl radical are higher than the aryl cation and the free energies of the final products show biphenyl as slightly more stable than phenol. Therefore, based on the experimental data and the computational analysis, we believe that the most plausible reaction mechanism for the metal-free photochemically-activated cross coupling follows a cationic pathway (**Path B**), starting with the protonation of the triazene, followed by (*E*)-(*Z*) photoisomerization under UV light irradiation, which activates the triazene for decomposition into an aryldiazonium salt. This aryldiazonium ion loses nitrogen to generate an aryl cation which, in turn, can either react with an aromatic molecule to form the biaryl product or be captured by a molecule of water to produce the corresponding phenol. These two competitive processes which tend to slightly favour the phenolic product during the final step are likely the cause for the observed yields in our reactions and previous unexplained low yields reported in many different aryl-aryl cross couplings articles.^{15,26,28,52} Therefore, our studies are expected to positively impact similar transformations thus significantly helping to contribute to enhanced milder and more sustainable approaches in many chemical reactions and synthetic processes.

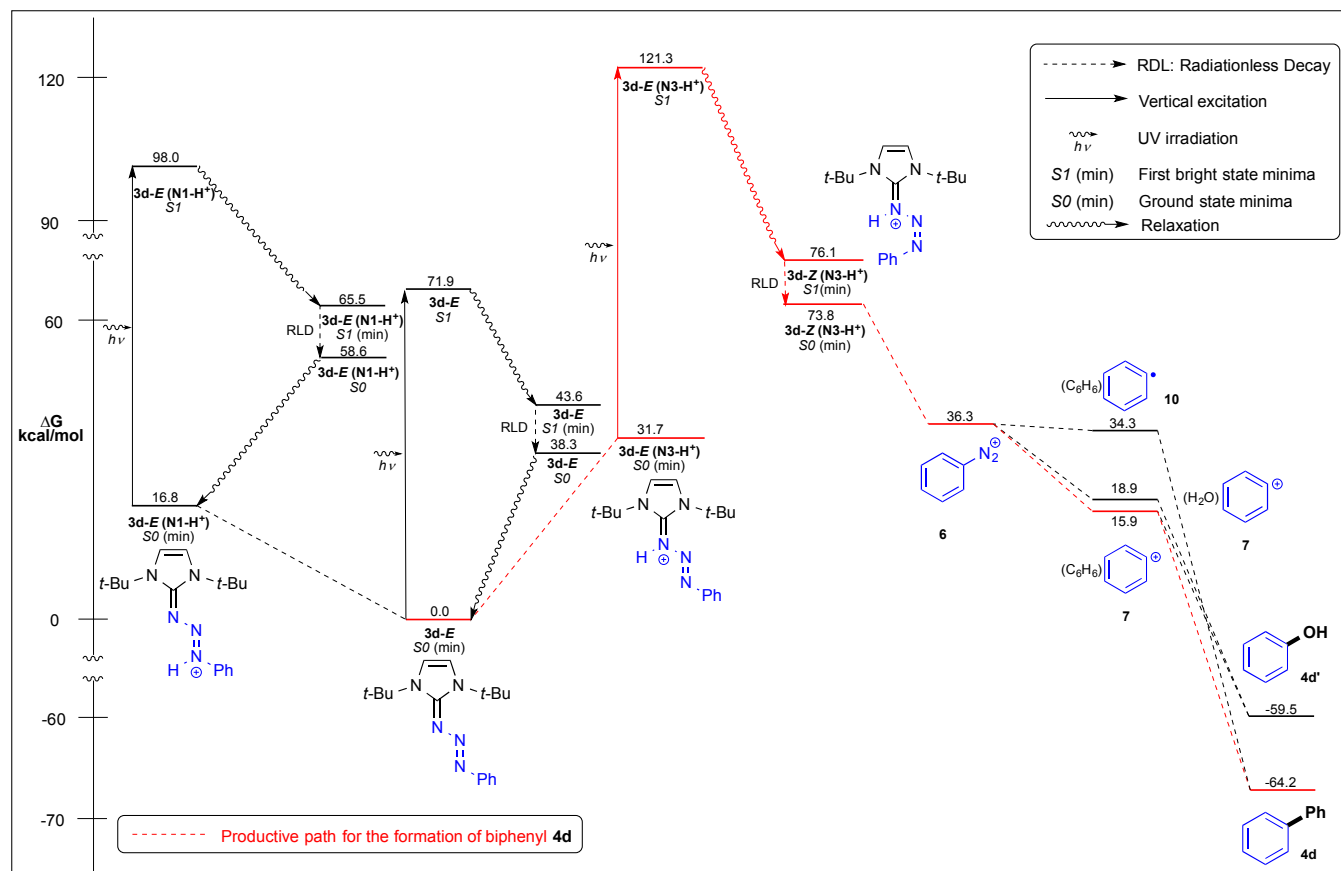


Figure 2 B3LYP/6-31G* Reaction energy diagram for the sp^2 - sp^2 cross-coupling of triazene **3d** to form biphenyl **4d**, and phenol **4d'**.

Experimental

General information

All photochemical reactions were carried out in quartz tubes using a Rayonet photochemical reactor with 350 nm UV lamps or stirred under natural sunlight. All commercially obtained reagents were used as received. Solvents were dried, degassed, and obtained from a JC Meyer company solvent purification system. Heating was accomplished by either a heating mantle or silicone oil bath. Purification of reaction products was carried out by flash column chromatography using silica gel 60 (230-400 mesh). TLC visualization was accompanied with UV light. Concentration *in vacuo* refers to the removal of volatile solvent using a rotary evaporator attached to a dry diaphragm pump (10-15 mm Hg) followed by pumping to a constant

weight with an oil pump (<300 mTorr). ^1H NMR spectra were recorded at 500 MHz and are reported relative to CDCl_3 (δ 7.26) or DMSO (δ 2.50). ^1H NMR coupling constants (J) are reported in Hertz (Hz) and multiplicities are indicated as follows: s (singlet), d (doublet), t (triplet), m (multiplet). Proton-decoupled ^{13}C NMR spectra were recorded at 125 MHz and reported relative to CDCl_3 (δ 77.0) or DMSO (δ 39.52). IR experiments were recorded with neat samples on a Bruker Alpha instruments fitted with diamond ATR sample plate. High-resolution (HR) mass spectra were recorded at the Shimadzu Center Laboratory for Biological Mass Spectrometry at UTA.

General procedure for the synthesis of triazenes (**3a-p**)

To a round-bottom flask containing 1,3-ditert-butylimidazolium tetrafluoroborate (1.1 mmol), potassium *tert*-butoxide (1.3 mmol) and dry THF was added (10 mL) under an Argon atmosphere. The resulting suspension was stirred for 15 minutes, followed by dropwise addition of the aromatic azide (1.1 mmol). The resulting mixture was left stirring at room temperature for 12 h. After this time, hexanes (10 mL) were added and the resulting solid precipitate filtered. The filtered solid was dissolved in DCM (20 mL) and the precipitated salts filtered. The resulting solution was then concentrated *in vacuo* and dried under high vacuum, affording pure triazenes.

General procedure for the synthesis of biaryls (4a-u)

To a quartz tube containing a triazene (0.2 mmol) was added the arene (2 mL). Then, the tube was capped and TFA (1.0 mmol) was added with a syringe. Next, the mixture was left to stir inside a photoreactor under UV irradiation (350 nm) for 2 h. After 2 h the resulting mixture was concentrated *in vacuo*. Purification by flash chromatography (SiO₂, EtOAc/hexanes mixtures) provided pure biaryl compounds. Alternatively, we also performed the experiment under the same conditions but using natural sunlight as our radiation source. These sunlight experiments were run in quartz tubes under natural sunlight for 9 h.

Procedure for the synthesis of immunosuppressant 5²⁷

To a round bottom flask equipped with a magnetic stir bar was added compound **4v** (0.2 mmol, 52 mg, 1.0 equiv), dipalladium(0) *tris*-dibenzylideneacetone (4 mol%, 8 mg), Me₃t-Bu-XPhos (6 mol%, 6 mg), potassium phosphate (0.3 mmol, 44 mg, 1.5 equiv) and 2,3-(difluoro)phenylformamide (0.2 mmol, 40 mg, 1.2 equiv). The flask was flushed with argon and 2 mL of *tert*-butanol were added, then the flask was sealed. The reaction mixture was then heated to 100 °C with constant stirring for 24 h. After this time, the reaction mixture was allowed to cool to room temperature, diluted with 20 mL of ethyl acetate, filtered through Celite and the resulting mixture was concentrated *in vacuo*. Purification by flash chromatography (SiO₂/EtOAc/hexane mixtures) provided the pure adduct as a white solid.

Conclusions

This work describes the first methodology for metal-free conversion of π -conjugated triazenes into synthetically useful biaryl compounds, at room temperature in only two hours. The approach also takes advantage of the power of photochemistry and the versatile properties of triazenes that generate aryldiazonium species *in situ* in a safe manner. Furthermore, this study allowed access to hetero- and biaryl adducts via cross-coupling of unactivated arenes. Therefore, this study provides a useful tool for constructing biaryl scaffolds by *in situ* generation of aryl cations. It also provides important theoretical and experimental mechanistic insights, results that should potentially open a new area of research with these compounds. It is important to note

that the reaction conditions are milder and more sustainable than those using stoichiometric amounts of toxic organometallic reagents, traditionally performed at higher temperatures in the presence of transition state metals. Additionally, this approach minimizes chemical wastes, and reduces cost, time, and separation of metallic impurities, while having the potential of simply using solar energy as light source. We hope, further studies, especially those aimed to mitigate the competitive process (phenol formation), will be positively impacted by our discoveries.

Conflicts of interest

There are no conflicts to declare.

Acknowledgements

A. B. is thankful to the University of Texas at Arlington for partially supporting this work. A.B. also acknowledge the ACS-PRF-ND grant (58261-ND1) for financial support. The Shimadzu Center for MS data collection and the NSF grants (CHE-0234811 and CHE-0840509) for additional instrumentation. H. W. acknowledges the support from the NSF Grant (CHE-1500285) and resources of the National Energy Research Scientific Computing Center, which is supported by the Office of Science of the U.S. Department of Energy under Contract No. DE-AC02-05CH11231.

Notes and references

1. A. Albin and M. Fagnoni, *ChemSusChem*, 2008, **1**, 63-66.
2. A. Albin and M. Fagnoni, *Green Chem.*, 2004, **6**, 1-6.
3. H. D. Roth, *Angew. Chem. Int. Ed.*, 1989, **28**, 1193-1207.
4. G. Ciamician, *Science*, 1912, **36**, 385-394.
5. P. Klán and J. Wirz, *Photochemistry of Organic Compounds*, John Wiley & Sons Ltd., 2009.
6. N. A. Romero and D. A. Nicewicz, *Chem. Rev.*, 2016, **116**, 10075-10166.
7. D. H. Waldeck, *Chem. Rev.*, 1991, **91**, 415-436.
8. T. Bach, *Synthesis*, 1998, **1998**, 683-703.
9. M. T. Crimmins, *Chem. Rev.*, 1988, **88**, 1453-1473.
10. P. Klán, T. Šolomek, C. G. Bochet, A. Blanc, R. Givens, M. Rubina, V. Popik, A. Kostikov and J. Wirz, *Chem. Rev.*, 2013, **113**, 119-191.
11. (a) L. Peng, Z. Li and G. Yin, *Org. Lett.*, 2018, **20**, 1880-1883; (b) X.-Y. Yu, J.-R. Chen, P.-Z. Wang, M.-N. Yang, D. Liang and W.-J. Xiao, *Angew. Chem. Int. Ed.*, 2018, **57**, 738-743.
12. J. Hassan, M. Sévignon, C. Gozzi, E. Schulz and M. Lemaire, *Chem. Rev.*, 2002, **102**, 1359-1470.
13. L. Ackermann, H. K. Potukuchi, A. Althammer, R. Born and P. Mayer, *Org. Lett.*, 2010, **12**, 1004-1007.
14. S. K. Gurung, S. Thapa, A. Kafle, D. A. Dickie and R. Giri, *Org. Lett.*, 2014, **16**, 1264-1267.
15. J. Han, Y. Liu and R. Guo, *J. Am. Chem. Soc.*, 2009, **131**, 2060-2061.
16. F. Y. Kwong, K. S. Chan, C. H. Yeung and A. S. C. Chan, *Chem. Commun.*, 2004, **0** 2336-2337.

17. E. Negishi, A. O. King and N. Okukado, *J. Org. Chem.*, 1977, **42**, 1821-1823.
18. E.-i. Negishi, *Angew. Chem. Int. Ed.*, 2011, **50**, 6738-6764.
19. X.-Q. Zhang and Z.-X. Wang, *J. Org. Chem.*, 2012, **77**, 3658-3663.
20. J.-H. Li, Y. Liang, D.-P. Wang, W.-J. Liu, Y.-X. Xie and D.-L. Yin, *J. Org. Chem.*, 2005, **70**, 2832-2834.
21. S. P. H. Mee, V. Lee and J. E. Baldwin, *Angew. Chem. Int. Ed.*, 2004, **43**, 1132-1136.
22. E. Alacid and C. Nájera, *J. Org. Chem.*, 2008, **73**, 2315-2322.
23. M. G. McLaughlin, C. A. McAdam and M. J. Cook, *Org. Lett.*, 2015, **17**, 10-13.
24. D. Friedman, T. Masciangioli and S. Olson, *The Role of the Chemical Sciences in Finding Alternatives to Critical Resources*, National Academy Press, 2012.
25. R. Dach, J. J. Song, F. Roschangar, W. Samstag and C. H. Senanayake, *Org. Process Res. Dev.*, 2012, **16**, 1697-1706.
26. A. Dewanji, S. Murarka, D. P. Curran and A. Studer, *Org. Lett.*, 2013, **15**, 6102-6105.
27. T. E. Storr and M. F. Greaney, *Org. Lett.*, 2013, **15**, 1410-1413.
28. J. Hofmann, E. Gans, T. Clark and M. R. Heinrich, *Chem. Eur. J.*, 2017, **23**, 9647-9656.
29. F. W. Wassmundt and W. F. Kiesman, *J. Org. Chem.*, 1997, **62**, 8304-8308.
30. R. Pazo-Llorente, H. Maskill, C. Bravo-Diaz and E. Gonzalez-Romero, *Eur. J. Org. Chem.*, 2006, **2006**, 2201-2209.
31. C. Galli, *Chem. Rev.*, 1988, **88**, 765-792.
32. J. P. Agrawal and R. Hodgson, *Organic Chemistry of Explosives*, John Wiley & Sons, Ltd., 2007.
33. S. Patil, K. White and A. Bugarin, *Tetrahedron Lett.*, 2014, **55**, 4826-4829.
34. S. Patil and A. Bugarin, *Acta Crystallogr. E*, 2014, **70**, 224-227.
35. S. Patil and A. Bugarin, *Eur. J. Org. Chem.*, 2016, **2016**, 860-870.
36. I. Fabre, L. A. Perego, J. Bergès, I. Ciofini, L. Grimaud and M. Taillefer, *Eur. J. Org. Chem.*, 2016, **2016**, 5887-5896.
37. F. W. Kimani and J. C. Jewett, *Angew. Chem. Int. Ed.*, 2015, **54**, 4051-4054.
38. J. He, F. W. Kimani and J. C. Jewett, *J. Am. Chem. Soc.*, 2015, **137**, 9764-9767.
39. D. C. Knyazeva, F. W. Kimani, J.-L. Blanche and J. C. Jewett, *Tetrahedron Lett.*, 2017, **58**, 2700-2702.
40. D. S. Roman, Y. Takahashi and A. B. Charette, *Org. Lett.*, 2011, **13**, 3242-3245.
41. D. M. Khramov and C. W. Bielawski, *J. Org. Chem.*, 2007, **72**, 9407-9417.
42. S. Caron, *Practical Synthetic Organic Chemistry*, John Wiley & Sons, Ltd., 2011
43. Y. H. Shao, Z. T. Gan, E. Epifanovsky, A. T. B. Gilbert, M. Wormit, J. Kussmann, A. W. Lange, A. Behn, J. Deng, X. T. Feng, D. Ghosh, M. Goldey, P. R. Horn, L. D. Jacobson, I. Kaliman, R. Z. Khaliullin, T. Kus, A. Landau, J. Liu, E. I. Proynov, Y. M. Rhee, R. M. Richard, M. A. Rohrdanz, R. P. Steele, E. J. Sundstrom, H. L. Woodcock, P. M. Zimmerman, D. Zuev, B. Albrecht, E. Alguire, B. Austin, G. J. O. Beran, Y. A. Bernard, E. Berquist, K. Brandhorst, K. B. Bravaya, S. T. Brown, D. Casanova, C. M. Chang, Y. Q. Chen, S. H. Chien, K. D. Closser, D. L. Crittenden, M. Diedenhofen, R. A. DiStasio, H. Do, A. D. Dutoi, R. G. Edgar, S. Fatehi, L. Fusti-Molnar, A. Ghysels, A. Golubeva-Zadorozhnaya, J. Gomes, M. W. D. Hanson-Heine, P. H. P. Harbach, A. W. Hauser, E. G. Hohenstein, Z. C. Holden, T. C. Jagau,
- H. J. Ji, B. Kaduk, K. Khistyayev, J. Kim, J. Kim, R. A. King, P. Klunzinger, D. Kosenkov, T. Kowalczyk, C. M. Krauter, K. U. Lao, A. D. Laurent, K. V. Lawler, S. V. Levchenko, C. Y. Lin, F. Liu, E. Livshits, R. C. Lochan, A. Luenser, P. Manohar, S. F. Manzer, S. P. Mao, N. Mardirossian, A. V. Marenich, S. A. Maurer, N. J. Mayhall, E. Neuscammann, C. M. Oana, R. Olivares-Amaya, D. P. O'Neill, J. A. Parkhill, T. M. Perrine, R. Peverati, A. Prociuk, D. R. Rehn, E. Rosta, N. J. Russ, S. M. Sharada, S. Sharma, D. W. Small, A. Sodt, T. Stein, D. Stuck, Y. C. Su, A. J. W. Thom, T. Tsuchimochi, V. Vanovschi, L. Vogt, O. Vydrov, T. Wang, M. A. Watson, J. Wenzel, A. White, C. F. Williams, J. Yang, S. Yeganeh, S. R. Yost, Z. Q. You, I. Y. Zhang, X. Zhang, Y. Zhao, B. R. Brooks, G. K. L. Chan, D. M. Chipman, C. J. Cramer, W. A. Goddard, M. S. Gordon, W. J. Hehre, A. Klamt, H. F. Schaefer, M. W. Schmidt, C. D. Sherrill, D. G. Truhlar, A. Warshel, X. Xu, A. Aspuru-Guzik, R. Baer, A. T. Bell, N. A. Besley, J. D. Chai, A. Dreuw, B. D. Dunietz, T. R. Furlani, S. R. Gwaltney, C. P. Hsu, Y. S. Jung, J. Kong, D. S. Lambrecht, W. Z. Liang, C. Ochsenfeld, V. A. Rassolov, L. V. Slipchenko, J. E. Subotnik, T. Van Voorhis, J. M. Herbert, A. I. Krylov, P. M. W. Gill and M. Head-Gordon, *Mol. Phys.*, 2015, **113**, 184-215.
44. V. Barone and M. Cossi, *J. Phys. Chem. A*, 1998, **102**, 1995-2001.
45. M. Cossi, N. Rega, G. Scalmani and V. Barone, *J. Comput. Chem.*, 2003, **24**, 669-681.
46. M. Feyereisen, G. Fitzgerald and A. Komornicki, *Chem. Phys. Lett.*, 1993, **208**, 359-363.
47. B. I. Dunlap, *Phys. Chem. Chem. Phys.*, 2000, **2**, 2113-2116.
48. Y. Jung, A. Sodt, P. M. W. Gill and M. Head-Gordon, *Proceedings of the National Academy of Sciences of the United States of America*, 2005, **102**, 6692-6697.
49. R. J. Cave and M. D. Newton, *J. Chem. Phys.*, 1997, **106**, 9213-9226.
50. R. J. Cave and M. D. Newton, *Chem. Phys. Lett.*, 1996, **249**, 15-19.
51. H. H. Hodgson, *Chem. Rev.*, 1947, **40**, 251-277.
52. J. R. Beadle, S. H. Korzeniowski, D. E. Rosenberg, B. J. Garcia-Slanga and G. W. Gokel, *J. Org. Chem.*, 1984, **49**, 1594-1603.